2

Geometrical Detection Algorithm for MIMO Systems

Z. Y. Shao, S. W. Cheung and T. I. Yuk
Department of Electrical and Electronic Engineering, The University of Hong Kong
Hong Kong SAR,
China

1. Introduction

The channel capacity and error-rate performance of MIMO systems could be improved by increasing the number of transmit antennas and receive antennas and the size of constellation used for modulation (Foschini and Gans, 1998). A main bottleneck that restricts the practical application of MIMO system is the unsatisfactory performance of the decoding algorithms, due to either high computational complexity required or poor symbol error-rate (SER) performance. Maximum-likelihood (ML) decoding which employs an exhaustive search strategy under the minimum Euclidean-distance principle can exploit all the available diversity and provide the optimum SER performance. However, its complexity increases exponentially with the number of antennas and the size of constellation used. Thus, for many cases, it is impractical to implement. Several sub-optimum decoding algorithms such as equalization-based zero-forcing (ZF) and minimum-mean-square-error (MMSE) detectors and nulling-and-cancelling detectors (NC) have been proposed for MIMO systems (Paulraj, Nabar and Gore, 2003). Although their computation complexities are dramatically less, these decoding algorithms have severe degradations in SER performances. Sphere decoding (SD) (Viterbo and Boutros, 1999) is another search-based algorithm. Unlike the exhaustive search engaged in ML decoding, SD confines the searching zone to be inside some hyper sphere constructed in the space spanned by the received lattice points. It can offer optimum SER performance with reasonable complexity. Several searching strategies such as Fincke-Pohst (Fincke and Pohst, 1985) and Schnorr-Euchner (Schnorr and Euchner, 1994) have been developed to further improve the searching efficiency in SD.

Since the minimum Euclidean-distance principle could result in an optimum SER performance, the purpose of this chapter is to introduce another perspective of reconsidering this principle from the transmit lattice space. In the space spanned by the transmit lattice points, the Euclidean distance in ML decoding is found to be related to a series of concentric hyper ellipsoids. Searching the lattice point with the minimum Euclidean distance from the received signal vector is equivalent to searching the lattice point that is passed through by the smallest hyper ellipsoid. Decoding algorithms following this perspective are often called geometrical detection (Artes, Seethaler and Hlawatsch, 2003). In this Chapter, the geometrical analysis of signal decoding for MIMO channels is presented. Then, the ellipsoid searching decoding algorithm (Shao, Cheung and Yuk, 2009) is described. It is an add-on detection algorithm to standard suboptimal detection schemes

and has better error-rate performance and higher diversity gains than the standard suboptimal detection schemes.

2. Geometrical analysis of signal decoding for MIMO channels

Consider an uncoded MIMO system with M_T transmit antennas and M_R receive antennas over a fading channel. The received signal matrix is given by:

$$\hat{\mathbf{r}} = \hat{\mathbf{H}}\hat{\mathbf{x}} + \hat{\mathbf{n}} \tag{1}$$

where $\hat{\mathbf{r}} \in \mathbb{C}^{M_R}$ is the M_R-dimensional received signal vector, $\hat{\mathbf{x}} \in \mathbb{C}^{M_T}$ is the M_T-dimensional transmitted signal vector, $\hat{\mathbf{H}} \in \mathbb{C}^{M_R \times M_T}$ is the channel matrix and is assumed to be known at the receiver, and $\hat{\mathbf{n}} \in \mathbb{C}^{M_R}$ is an independently and identically distributed (i.i.d.) zero-mean Gaussian noise vector with elements having a fixed variance. Equation (1) represents a complex transmission, and it can be transformed into a real matrix equation:

$$\begin{bmatrix} \mathbf{Re}(\mathbf{r}) \\ \mathbf{Im}(\mathbf{r}) \end{bmatrix} = \begin{bmatrix} \mathbf{Re}(\mathbf{H}) & \mathbf{-Im}(\mathbf{H}) \\ \mathbf{Im}(\mathbf{H}) & \mathbf{Re}(\mathbf{H}) \end{bmatrix} \begin{bmatrix} \mathbf{Re}(\mathbf{x}) \\ \mathbf{Im}(\mathbf{x}) \end{bmatrix} + \begin{bmatrix} \mathbf{Re}(\mathbf{n}) \\ \mathbf{Im}(\mathbf{n}) \end{bmatrix} \tag{2}$$
$$\mathbf{r} = \mathbf{H}\mathbf{x} + \mathbf{n}$$

where $\mathbf{r} \in \mathbb{R}^{N_R}$, $\mathbf{x} \in \mathbb{R}^{N_T}$, $\mathbf{H} \in \mathbb{R}^{N_R \times N_T}$ and $\mathbf{n} \in \mathbb{R}^{N_R}$.
In ML decoding, the optimal solution is given by:

$$\mathbf{x}_{ML} = \arg\min_{\mathbf{s} \in \Omega} \left\| \mathbf{r} - \mathbf{H}\mathbf{s} \right\|^2 \tag{3}$$

where Ω is the set of all the possible transmitted signal vectors, and the term $\left\| \mathbf{r} - \mathbf{H}\mathbf{s} \right\|^2$ is known as the Euclidean distance between the received vector and the transmitted vector distorted by the channel matrix.
The Euclidean distance in ML decoding can be rewritten as:

$$f(\mathbf{s}) = \left\| \mathbf{r} - \mathbf{H}\mathbf{s} \right\|^2 = (\mathbf{s} - \mathbf{x}_c)^{\mathbf{H}} \mathbf{M}^{-1} (\mathbf{s} - \mathbf{x}_c) \tag{4}$$

where $\mathbf{M} = (\mathbf{H}^{\mathbf{T}}\mathbf{H})^{-1}$ and $\mathbf{x}_c$ is the result of zero-forcing (ZF) equalization (Wolniansky, Foschini, Golden and Valenzuela, 1998) and can be written as:

$$\mathbf{x}_c = (\mathbf{H}^T\mathbf{H})^{-1} \mathbf{H}^T\mathbf{r} = \mathbf{x} + (\mathbf{H}^T\mathbf{H})^{-1} \mathbf{H}^T\mathbf{n} = \mathbf{x} + \tilde{\mathbf{n}} \tag{5}$$

where $(\mathbf{H}^T\mathbf{H})^{-1} \mathbf{H}^T\mathbf{n} = \tilde{\mathbf{n}}$. Substituting (4) into (3) yields:

$$\mathbf{x}_{ML} = \arg\min_{\mathbf{s} \in \Omega} \left\{ (\mathbf{s} - \mathbf{x}_c)^T \mathbf{H}^T\mathbf{H} (\mathbf{s} - \mathbf{x}_c) \right\} \tag{6}$$

It can be seen from (5) and (6) that, in the absence of noise or equivalently the transformed Gaussian noise term $\tilde{\mathbf{n}} = (\mathbf{H}^T\mathbf{H})^{-1} \mathbf{H}^T\mathbf{n}$, both ZF detector and ML decoding will result in the same correct solution. The reason why ML decoding can offer much better SER performance

than ZF lies on the fact that the transformed Gaussian noise has been minimized by the exhaustive search used in ML decoding, but the ZF results are directly distorted by the transformed Gaussian noise $\tilde{\mathbf{n}}$.

Using eigenvalue decomposition, the matrix $\mathbf{M}$ in (4) can be decomposed as:

$$\mathbf{M} = \left(\mathbf{H}^{\mathrm{T}}\mathbf{H}\right)^{-1} = \mathbf{V}\Lambda\mathbf{V}^{\mathrm{T}} \tag{7}$$

where $\Lambda = diag\left(\lambda_1, \lambda_2, ..., \lambda_{M_T}\right) \in \mathbb{R}^{N_T \times N_T}$ are the eigenvalues of $\mathbf{M}$ arranged in descending order, and $\mathbf{V} = \left[\mathbf{V}_1, \mathbf{V}_2, \cdots, \mathbf{V}_{M_T}\right] \in \mathbb{R}^{N_T \times N_T}$ is the corresponding eigenvector matrix (Samuel and Fitz, 2007).

In ML decoding, the Euclidean distance function $f(\mathbf{s})$ given in (4) geometrically represents an elliptic paraboloid (Horn and Johnson, 1985) in an $N_T + 1$ dimensional space with its axis perpendicular to an N_T dimensional subspace spanned by the symbol vectors in Ω. $\mathbf{x}_c$ is the global minimum point of the elliptic paraboloid and is located on the subspace spanned by the symbol vectors in Ω as shown in Fig. 1. It can be seen from (4) that the function $f(\mathbf{s})$ reaches its minimum value at $\mathbf{x}_c$,i.e., $f(\mathbf{s})_{\min} = f(\mathbf{x}_c) = 0$. The horizontal cross-section of the elliptic paraboloid (4) is an N_T dimensional hyper ellipsoid given by:

$$f(\mathbf{s}) = a^2 \tag{8}$$

where a^2 represents the height of the cross section above the N_T dimensional space as shown in Fig. 1. The length and direction of *i*-th semiaxis of the hyper ellipsoid are given as $a\sqrt{\lambda_i}$ and $\mathbf{V}_i$, respectively. With different values of a^2, a series of concentric hyper

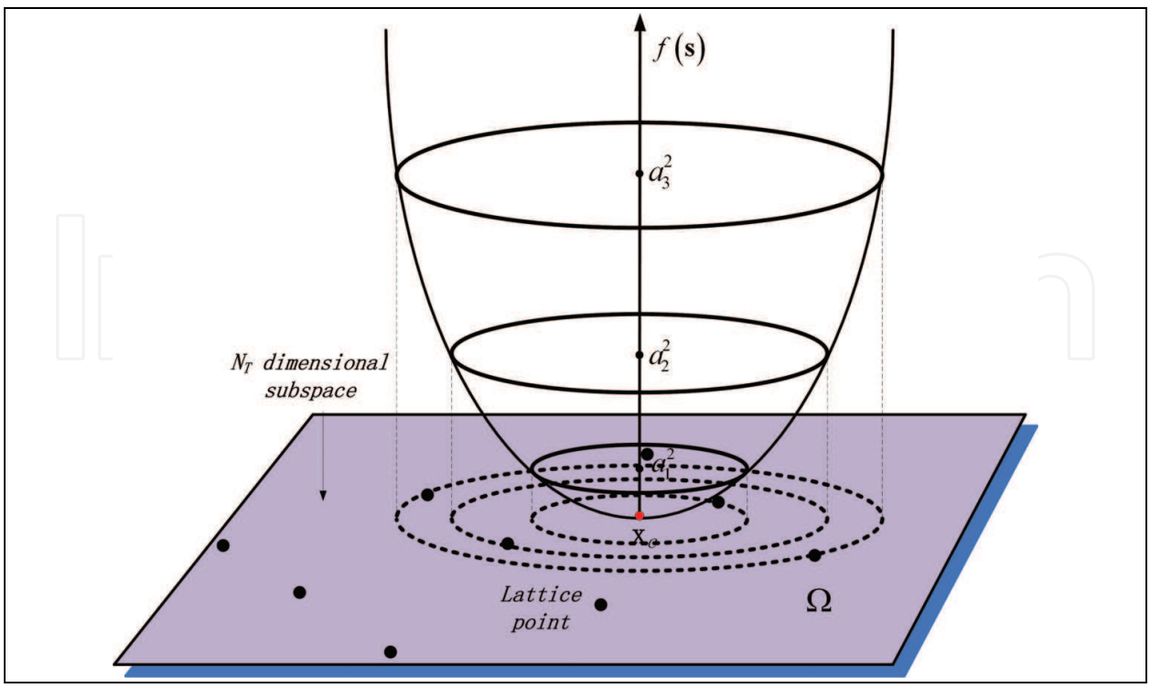

Fig. 1. Elliptic paraboloid with axis perpendicular to a subspace spanned by lattice points.

ellipsoids are obtained and can be projected onto the subspace spanned by the vectors as shown by the dash lines in Fig. 1. Thus, searching the lattice point with minimum Euclidean distance is equivalent to searching the lattice point that is passed through by the smallest hyper ellipsoid.

3. Ellipsoid-searching decoding algorithm

From section **2,** we know that $f(\mathbf{s}) = a^2$ represents a hyper ellipsoid centered at point $\mathbf{x_c}$ with the length and direction of its *i*-th semiaxis given as $a\sqrt{\lambda_i}$ and $\mathbf{v}_i$, respectively. By choosing different values of a, a group of similar hyper ellipsoids can be obtained. Thus, the solution of ML decoding must be located on a hyper ellipsoid which has the minimum surface area among these similar hyper ellipsoids.

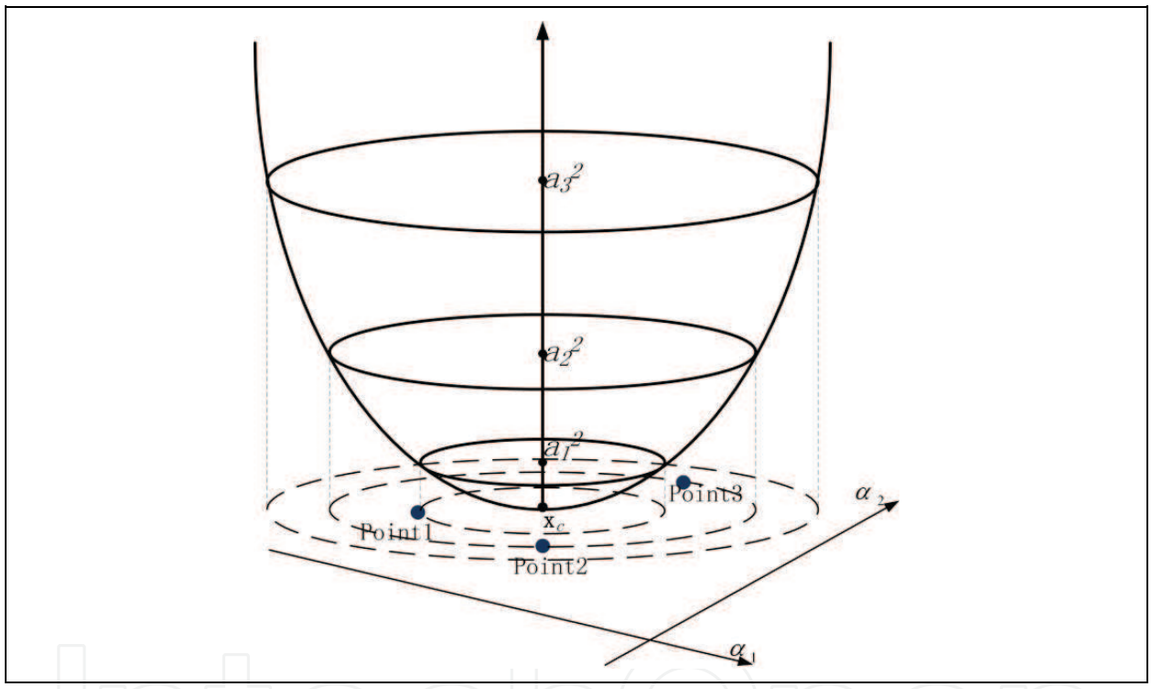

Fig. 2. Elliptic paraboloid in 3-dimensional space.

Fig. 2 shows a two dimensional lattice point space ($\alpha_1 - \alpha_2$ plane) with three lattice points Point 1, Point 2, and Point 3 as shown in the figure. With different a^2, a group of similar hyper ellipsoids can be obtained, and their projection onto the $\alpha_1 - \alpha_2$ plane are ellipses which are all centered at the point $\mathbf{x}_c$. For each lattice point, there exists an ellipse that passes through it. The corresponding ellipse of the ML solution is the one that has the minimum area. As shown in Fig. 2, Point 1 is taken to be the ML solution while Point 2 and Point 3 are not, since it is the inner-most ellipse and thus has the minimum area.

However, finding the smallest hyper ellipsoid containing the solution signal vector is not an easy task. If we use the largest hyper ellipsoid which contains all the signal vectors, then the complexity will be the same as ML decoding. Here we propose an ellipsoid-searching decoding algorithm (ESA) that uses a small hyper ellipsoid containing the solution symbol

vector to start the search and then identify all the symbol vectors inside. The ESA consists of the following 3 steps:

3.1 Start with zero-forcing points

It is well known that zero-forcing (ZF) decoding is one form of linear equalization algorithm. Although it cannot offer very high performance like ML decoding, its solution however usually lies in the neighborhood of the transmit signal point. Thus we can consider choosing the hyper ellipsoid that goes through the ZF solution to start the search. First, the ZF equalized $\mathbf{x}_{zf}$ is solved. Then its corresponding a_{zf}^2 is computed. The starting hyper ellipsoid is obtained as:

$$f\left(\mathbf{x}_{zf}\right) = a_{zf}^2 \tag{9}$$

3.2 Determine a circumscribed hyper rectangle

After determining the hyper ellipsoid, the next key task is to identify whether there are any lattice points located inside this hyper ellipsoid. The axes of the N_T-dimensional rectangular coordinate system for the lattice point space are denoted as α_i- axes. Since the directions of the hyper ellipsoid's semiaxes are not in parallel with the axes of the coordinate system of the lattice point space, it is rather complicated to directly use the surface equation (9) of the hyper ellipsoid. Here we propose to use a circumscribed hyper rectangle as follows.

We set up a new N_T-dimensional rectangular coordinate system with α_i'- axes ($i = 1,2,3,...,N_T$) which coincide with the *i*-th semiaxis of the hyper ellipsoid and has the origin coincides with the global minimum point $\mathbf{x_c}$. We use the superscript prime to denote the variables in the new coordinate system. The coordinates of the 2^{N_T} apexes of the circumscribed hyper rectangle in this new coordinate system are given by:

$$k_p{}' = \left[x'_{p1}, x'_{p2}, ...x'_{pN_T} \right] \tag{10}$$

where $p = 1,2,3,...2^{N_T}$, $x'_{pj} = \pm a_{zf}\sqrt{\lambda_j}$, and a_{zf} is related to the hyper ellipsoid given by (9). It can be easily shown that, by using coordinate transformation, the coordinates of the 2^{N_T} apexes in the original lattice point space are:

$$\mathbf{k}_p^T = \mathbf{V} \cdot \left(\mathbf{k}'_p\right)^T + \mathbf{x}_c \tag{11}$$

where $\mathbf{V}$ is the eigenvector matrix in (7), and it serves as the transformation matrix:

$$\mathbf{V}_T = \left[\mathbf{V}_1, \mathbf{V}_2, \cdots, \mathbf{V}_{N_T} \right] = \begin{bmatrix} v_{11} & v_{21} & v_{31} & \cdots & v_{N_T 1} \\ v_{12} & v_{22} & v_{32} & \cdots & v_{N_T 2} \\ v_{13} & v_{23} & v_{33} & \cdots & v_{N_T 3} \\ \vdots & \vdots & \vdots & \ddots & \vdots \\ v_{1N_T} & v_{2N_T} & v_{3N_T} & \cdots & v_{N_T N_T} \end{bmatrix} \tag{12}$$

Thus the value of the *i*-th component of $\mathbf{k}_p$ can be obtained as:

$$x_{pi} = \sum_{q=1}^{N_T} \left(v_{qi} x'_{pq} \right) + x_{ci} \tag{13}$$

where x_{ci} is the *i*-th component of $\mathbf{x_c}$. Since $x'_{pq} = a_{zf}\sqrt{\lambda_q}$, the maximum and minimum boundaries in the α'_i - axes for each component in $\mathbf{k}_p$ can be expressed as:

$$x_{i\_\max} = x_{ci} + \sum_{q=1}^{N_T} \left| v_{qi} a_{zf} \sqrt{\lambda_q} \right| \tag{14.1}$$

$$x_{i\_\min} = x_{ci} - \sum_{q=1}^{N_T} \left| v_{qi} a_{zf} \sqrt{\lambda_q} \right| \tag{14.2}$$

Since the circumscribed hyper rectangle encloses the hyper ellipsoid, so any lattice point $\mathbf{s} = \begin{bmatrix} s_1 & s_2 & \dots & s_{N_T} \end{bmatrix}$ inside the hyper ellipsoid satisfies:

$$x_{i\_\min} < s_i < x_{i\_\max} \qquad i = 1, 2, 3, \dots, N_T \tag{15}$$

It should be noted that this is not a sufficient condition for identifying the lattice points lying inside the hyper ellipsoid.

From (15), we can obtain the possible value set $\xi_i = \{\varepsilon_{i1}, \varepsilon_{i2}, \varepsilon_{i3}, \cdots\}$ for the *i*-th element of the lattice points located inside the hyper ellipsoid. So the search set becomes a larger hyper rectangle that encloses the circumscribed hyper rectangle. For PAM and QAM, the elements of ξ_j are the odd numbers between $x_{j\_\max}$ and $x_{j\_\min}$, and it can be easily shown that the number of elements is:

$$Num_i = \left\lfloor \sum_{q=1}^{N_T} \left| v_{qi} a_{zf} \sqrt{\lambda_q} \right| \right\rfloor \tag{16}$$

3.3 Narrow the search set into ellipsoid

As mentioned before, the search set becomes a larger hyper rectangle and the number of lattice points inside is $\prod_{i=1, i\neq l}^{N_T} Num_i$. If there is any Num_i equals zero, then it means that there is no lattice point located inside the hyper ellipsoid. The searching process will terminate and the zero forcing point chosen before is considered as the solution.

Otherwise, assuming the possible value set ξ_ω has the largest number of elements among all the possible value sets, we form the combinations from the other $N_T - 1$ possible value sets, and then substitute each of these combinations into (9), to determine the lattice point elements of the possible value set ξ_ω that are located inside the hyper ellipsoid. In doing so,

the number of combinations that need to be considered is smaller and hence lesser computation complexity. Denoting the *k*-th combination by:

$$\mathbf{Com}^k = \left[\varepsilon_{1,k}, \varepsilon_{2,k}, \cdots \varepsilon_{\omega-1,k}, \varepsilon_{\omega+1,k} \cdots, \varepsilon_{N_T,k} \right] \tag{17}$$

$$k = 1, 2, ..., \prod_{j=1, j\neq\omega}^{N_T} Num_j$$

where $\varepsilon_{j,k}$ represents an arbitrary element of the set ξ_j.

Geometrically, the $\mathbf{Com}^k$ is a line pierced through the hyper ellipsoid. The intersection of the line and the hyper ellipsoid consists of two points, known as $E_{\max,k}$ and $E_{\min,k}$ along the ω-th axis. Hence, the corresponding possible value set $\zeta_{\omega,k} = \left\{ \varsigma_{\omega,1,k}, \varsigma_{\omega,2,k}, ... \right\}$ for the ω-th element of the lattice points are the odd numbers between $E_{\max,k}$ and $E_{\min,k}$. Thus, any lattice point that is located inside the hyper ellipsoid can be expressed as:

$$\mathbf{x}_{d,k} = \left[\varepsilon_{1,k}, \varepsilon_{2,k}, \cdots \varepsilon_{\omega-1,k}, \varsigma_{\omega,d,k}, \varepsilon_{\omega+1,k} \cdots, \varepsilon_{N_T,k} \right]^T \tag{18}$$

$$d = 1, 2, ..., n_k$$

where n_k is the number of the elements of $\zeta_{\omega,k}$ for $\mathbf{Com}^k$.

Finally, we calculate the corresponding a^2 of each lattice point $\mathbf{x}_{d,k}$ by (8). The point with the minimum a^2 is the solution.

3.4 Examples

a. 2-D lattice space

For a 2×2 8-PAM MIMO system, the lattice set is a 2-dimensional space as shown in Fig. 3, where it is assumed that the ellipse and its circumscribed rectangle have been determined using our proposed method as described previously. The semiaxes of the ellipse are in parallel with vectors $\mathbf{V}_1$ and $\mathbf{V}_2$ with lengths $a_{zf}\sqrt{\lambda_1}$ and $a_{zf}\sqrt{\lambda_2}$, respectively. The global minimum point $\mathbf{x}_c$ is marked by a triangle on the figure. The coordinates of the four apexes, *A*, *B*, *C* and *D*, in the new coordinate system are given by $A = \left(-a_{zf}\sqrt{\lambda_1}, -a_{zf}\sqrt{\lambda_2} \right)$, $B = \left(-a_{zf}\sqrt{\lambda_1}, +a_{zf}\sqrt{\lambda_2} \right)$, $C = \left(a_{zf}\sqrt{\lambda_1}, -a_{zf}\sqrt{\lambda_2} \right)$, and $D = \left(a_{zf}\sqrt{\lambda_1}, +a_{zf}\sqrt{\lambda_2} \right)$, respectively. Substituting these vectors into (13) yields the corresponding coordinates in the lattice point space. From (14), the $\mathbf{x}_1$ coordinates of points *A* and *D* are chosen as $x_{1\_\min}$ and $x_{1\_\max}$, respectively, and the $\mathbf{x}_2$ coordinates of points *B* and *C* are chosen as $x_{2\_\min}$ and $x_{2\_\max}$, respectively. Using (15), we can obtain a possible set of values along each axis, i.e., two values {1, 3} along the $\mathbf{x}_1$-axis and one value {1} along the $\mathbf{x}_2$-axis. Since the number of values along the $\mathbf{x}_1$-axis is larger than that along the $\mathbf{x}_2$-axis, we substitute $\varepsilon_{2,1} = 1$ into the hyper ellipsoid equation (9). As shown in Fig. 3, the possible value along the $\mathbf{x}_1$-axis is $\varsigma_{1,1,1} = 3$, so the point $\mathbf{x}_{1,1} = [3 \quad 1]^T$ is obtained. Since it is the only point located inside the ellipse, it would be the final solution.

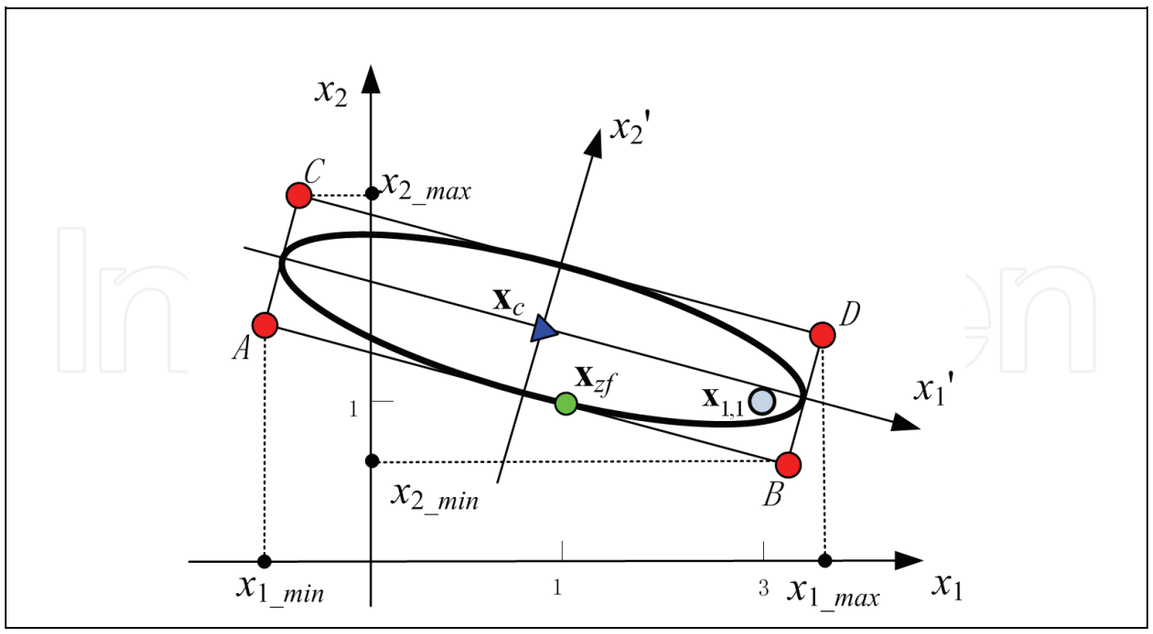

Fig. 3. 2-D lattice space example

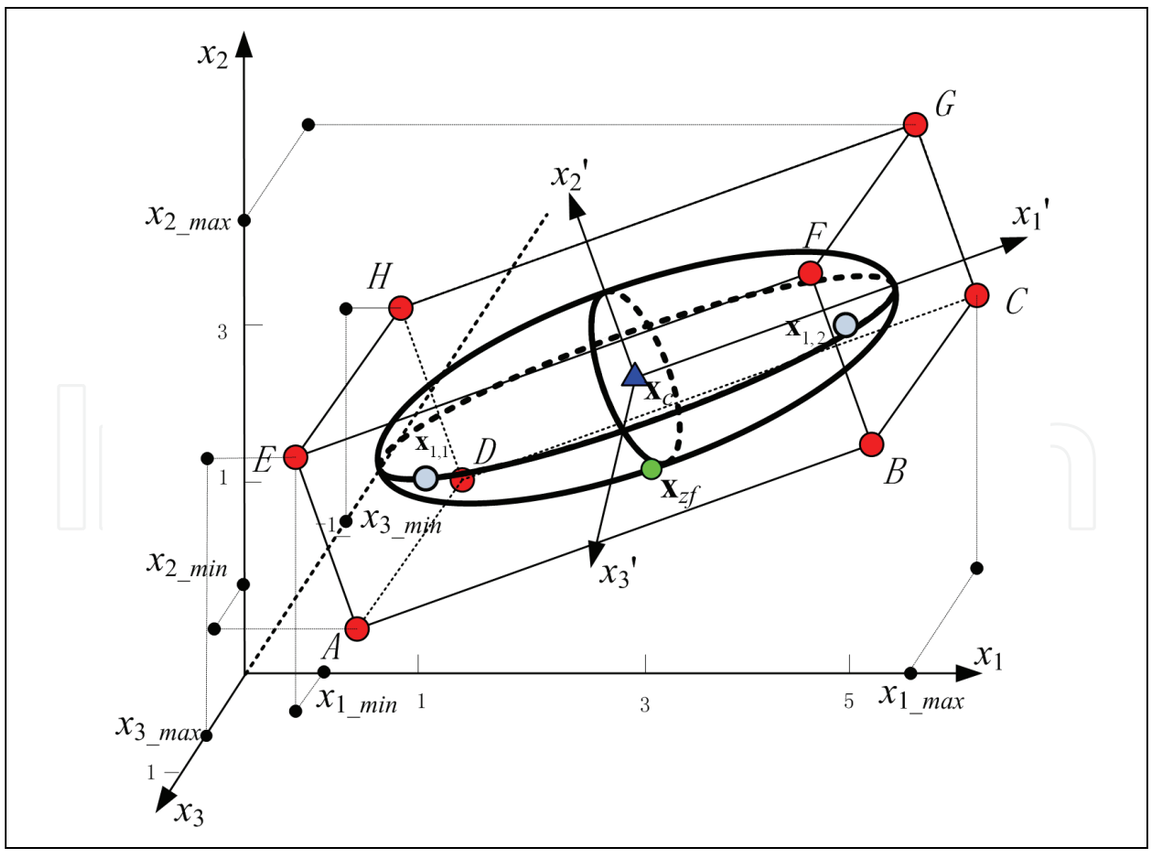

Fig. 4. 3-D lattice space example

b. 3-D lattice space

Here, we continue to consider the case of 3-dimensional lattice space, namely 3×3 8-PAM. Fig. 4 shows a 3-dimensional ellipsoid with its circumscribed rectangle which has been set up by the method introduced in section 3.2. $\mathbf{x}_c$ is the center of the ellipsoid, whose semiaxes are aligned along vectors $\mathbf{V}_1$, $\mathbf{V}_2$, $\mathbf{V}_3$, with their lengths being $a_{zf}\sqrt{\lambda_1}$, $a_{zf}\sqrt{\lambda_2}$ and $a_{zf}\sqrt{\lambda_3}$, respectively. By substituting the coordinates of the eight points *A* to *H* to (13) and (14), the boundary points $x_{1\_\min}$ and $x_{1\_\max}$, $x_{2\_\min}$ and $x_{2\_\max}$, $x_{3\_\min}$ and $x_{3\_\max}$, which are all marked as dots, are obtained. The possible set of values along $\mathbf{x}_1$-axis is {1, 3, 5}, and the possible set of values along the $\mathbf{x}_2$-axis is {1, 3}. Along $\mathbf{x}_3$-axis, the possible set of value is {-1}. Since the number of possible values along the $\mathbf{x}_1$-axis is the largest compared to those along the other axes, we substitute $\mathbf{Com}^1 = \left[\varepsilon_{2,1}, \varepsilon_{3,1}\right] = \left[1, -1\right]$ and $\mathbf{Com}^2 = \left[\varepsilon_{2,2}, \varepsilon_{3,2}\right] = \left[3, -1\right]$ into (9) to determine $E_{\max,k}$ and $E_{\min,k}$ along the $\mathbf{x}_1$-axis. As shown in Fig. 4, the possible value set $\zeta_{1,1}$ along the $\mathbf{x}_1$-axis is {1} for $\mathbf{Com}^1$ and $\zeta_{1,2}$ is {5} for $\mathbf{Com}^2$, so the point $\mathbf{x}_{1,1} = \left[1 \quad 1 \quad -1\right]^T$ and the point $\mathbf{x}_{1,2} = \left[5 \quad 3 \quad -1\right]^T$ are obtained. By calculating their corresponding a^2, it can be concluded that the point $\mathbf{x}_{1,2}$ that has a smaller a^2 is taken as the final solution.

3.5 Results and conclusion

The ESA algorithm for MIMO systems has been briefly introduced. It contains three main steps: Firstly, determine the hyper ellipsoid. Secondly, find out the probable value sets for each component of the lattice point that is located in the hyper ellipsoid. Finally, search for the ML solution. In the first step, either ZF detector or MMSE detector can be selected for determining the hyper ellipsoid. In the second step, we firstly determine a loose boundary for each component of the lattice points that may be located in the hyper ellipsoid. Then, by further shrink the value set of the N_T-th component, all the redundant points can be discarded and the lattice points inside the hyper ellipsoid are exactly detected.

Since the ESA algorithm uses the same criteria (3) of ML to make decision, it can thus achieve the same performance as ML decoding. However, the ML decoding searches the entire lattice space for solution while the ESA algorithm only searches a smaller subset, thus ESA is more computation efficient. Simulation results of various algorithms on the error rate performance are shown in Fig. 5 and Fig. 6 for comparison. In the simulations, we used 4-QAM, 16-QAM , 64-QAM in Rayleigh flat fading Channels with i.i.d. complex zero-mean Guassian noise. Fig. 5 illustrates the SER performance of ESA compared with ML decoding, ZF detector and MMSE detector using 4-QAM. Fig. 6 shows the SER performance of ESA compared with ML decoding ZF detector and MMSE detector using 16-QAM and 64-QAM. The performances of ESA can achieve the same performance as the ML decoding and are much better than the sub-optimum detectors.

4. Conclusion

In this chapter, the geometrical analysis of signal decoding for MIMO channels is presented. The ellipsoid searching decoding algorithm using geometrical approach is introduced. It is an add-on to standard suboptimal detection schemes and has better SER performance and higher diversity gains compared to the standard suboptimal detection schemes. It is able to provide the same optimum SER performance as in the ML decoding but with less complexity as only a subset of the lattice points are examined.

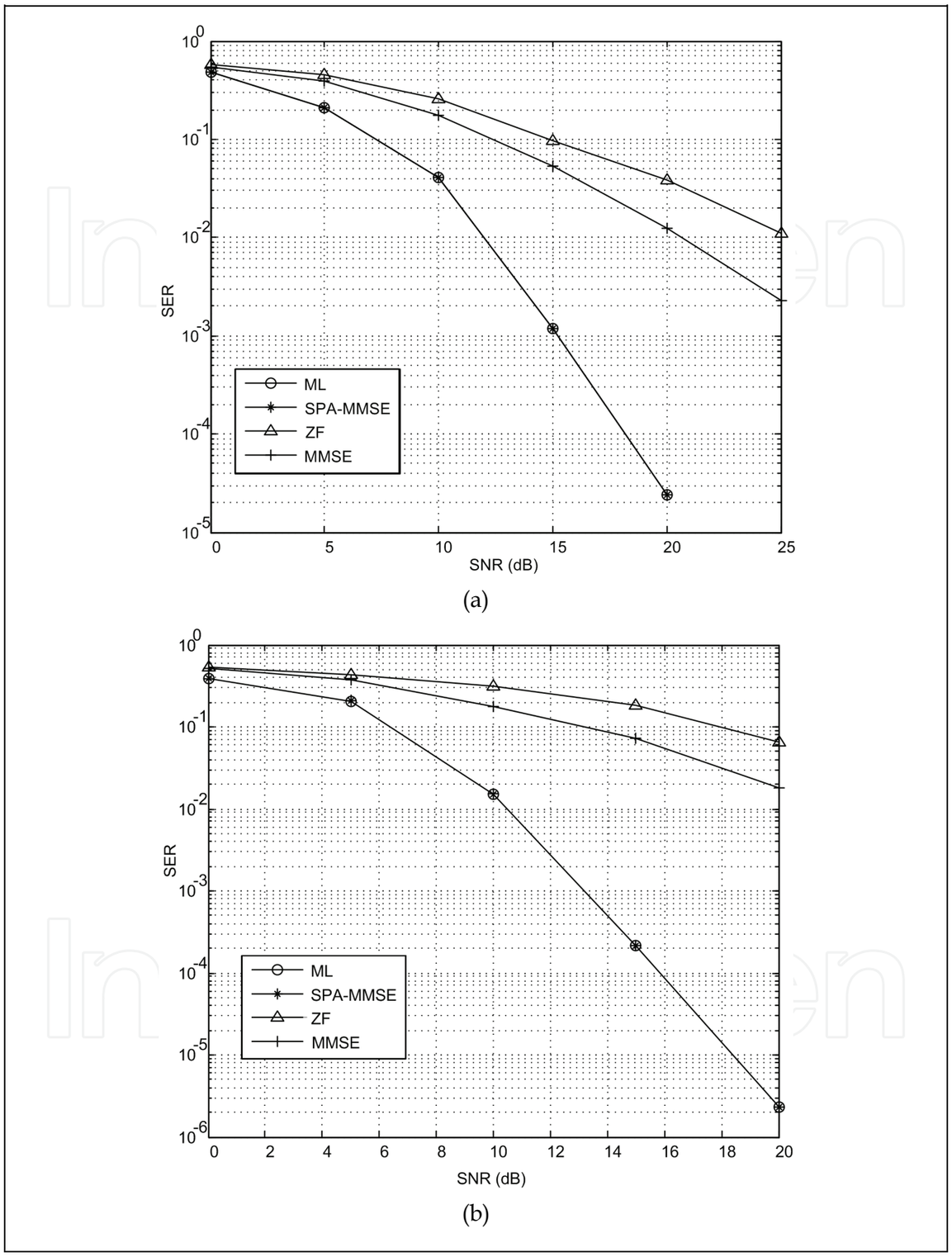

Fig. 5. Comparison of SER performance of ESA, ML decoding, ZF and MMSE using 4-QAM. (a) 4×4 MIMO systems. (b) 6×6 MIMO systems.

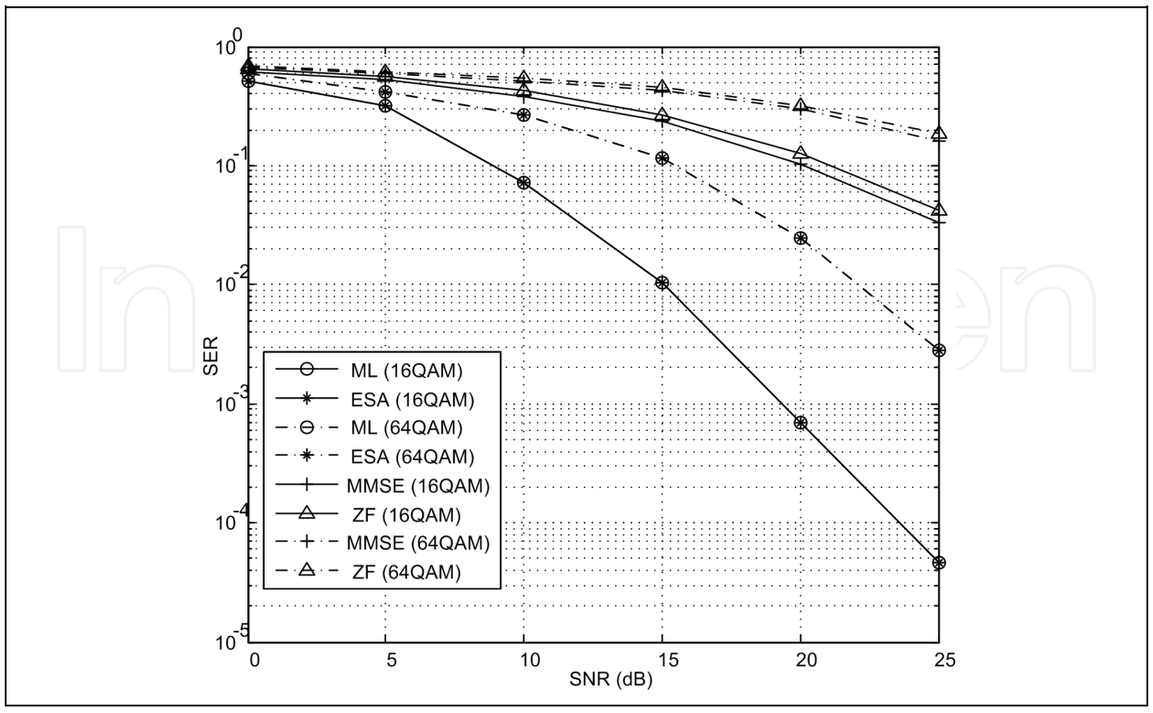

Fig. 6. Comparison of SER performance of ESA, ML decoding, ZF and MMSE using 16-QAM and 64-QAM in 4×4 MIMO system.

5. References

Fincke, U. & Pohst, M. (1985). Improved methods for Calculating vectors of short length in a lattice, including a complexity analysis, *Math. Comput*., Vol. 44, (1985) pp.463-471, ISSN: 0025-5718

Horn R. A. and Johnson C. R. (1985). Matrix Analysis, *Cambridge University Press*, (1985) ISBN: 0-521-30586-1.

Schnorr, C.P. & Euchner, M. (1994). Lattice basis reduction: improved practical algorithms and solving subset sum problems, *Math. Program*., Vol. 66, No. 2, (1994) pp.181-191, ISSN: 0025-5610

Foschini, G. J. & Gans, M. J. (1998). On limits of wireless communications in a fading environment when using multiple antennas, *Wireless Personal Commun*., Vol. 6, (Mar. 1998) pp. 311-335, ISSN: 0929-6212

Wolniansky P., Foschini G. J., Golden G. & Valenzuela R. (1998). V-BLAST: an architecture for realizing very high data rates over the rich-scattering wireless channel, *International Symposium on Signals, Systems and Electronics ISSSE98*, pp. 295–300.

Viterbo, E. & Boutros, J. (1999). A Universal Lattice Code Decoder for Fading Channels," *IEEE Trans. Information Theory*, Vol. 45, No. 5, (July 1999) pp. 1639–1642, ISSN: 0018-9448.

Paulraj A.; Nabar R. & Gore D., (2003). Introduction to Space-Time Wireless Communications, *Cambridge University Press*, (May 2003), ISBN:0521826152.

Artes, H.; Seethaler, D. & Hlawatsch, F. (2003). Efficient detection algorithms for mimo channels: A geometrical approach to approximate ml detection, *IEEE Trans. Signal Processing*, Vol. 51, No. 11, (Nov. 2003) pp. 2808–2820, ISSN: 1053-587X.

Seethaler, D.; Artes, H. & Hlawatsch, F. (2003). Efficient Near-ML Detection for MIMO Channels: The Sphere-Projection Algorithm, GLOBECOM, pp. 2098–2093.

Samuel M. and Fitz M. P. (2007). Geometric Decoding Of PAM and QAM Lattices, in *Proc. IEEE Global Telecommunications Conf.*, , (Nov.2007), pp. 4247–4252.

Shao, Z. Y. ; Cheung, S. W. & Yuk, T. I. (2009). A Simple and Optimum Geometric Decoding Algorithm for MIMO Systems, *4th International Symposium on Wireless Pervasive Computing 2009*, Melbourne, Australia

MIMO Systems, Theory and Applications

Edited by Dr. Hossein Khaleghi Bizaki

ISBN 978-953-307-245-6
Hard cover, 488 pages
Publisher InTech
Published online 04, April, 2011
Published in print edition April, 2011

In recent years, it was realized that the MIMO communication systems seems to be inevitable in accelerated evolution of high data rates applications due to their potential to dramatically increase the spectral efficiency and simultaneously sending individual information to the corresponding users in wireless systems. This book, intends to provide highlights of the current research topics in the field of MIMO system, to offer a snapshot of the recent advances and major issues faced today by the researchers in the MIMO related areas. The book is written by specialists working in universities and research centers all over the world to cover the fundamental principles and main advanced topics on high data rates wireless communications systems over MIMO channels. Moreover, the book has the advantage of providing a collection of applications that are completely independent and self-contained; thus, the interested reader can choose any chapter and skip to another without losing continuity.

InTech Europe
University Campus STeP Ri
Slavka Krautzeka 83/A
51000 Rijeka, Croatia
Phone: +385 (51) 770 447
Fax: +385 (51) 686 166
www.intechopen.com

InTech China
Unit 405, Office Block, Hotel Equatorial Shanghai
No.65, Yan An Road (West), Shanghai, 200040, China
中国上海市延安西路65号上海国际贵都大饭店办公楼405单元
Phone: +86-21-62489820
Fax: +86-21-62489821

IntechOpen